



**HAL**  
open science

# The Fluid Mechanics of Cleaning and Decontamination of Surfaces

Julien R Landel, D. Ian Wilson

► **To cite this version:**

Julien R Landel, D. Ian Wilson. The Fluid Mechanics of Cleaning and Decontamination of Surfaces. Annual Review of Fluid Mechanics, 2021, 53 (1), pp.147-171. 10.1146/annurev-fluid-022820-113739 . hal-04651675

**HAL Id: hal-04651675**

**<https://hal.science/hal-04651675v1>**

Submitted on 17 Jul 2024

**HAL** is a multi-disciplinary open access archive for the deposit and dissemination of scientific research documents, whether they are published or not. The documents may come from teaching and research institutions in France or abroad, or from public or private research centers.

L'archive ouverte pluridisciplinaire **HAL**, est destinée au dépôt et à la diffusion de documents scientifiques de niveau recherche, publiés ou non, émanant des établissements d'enseignement et de recherche français ou étrangers, des laboratoires publics ou privés.

Copyright

# The Fluid Mechanics of Cleaning and Decontamination of Surfaces

Julien R. Landel,<sup>1</sup> and D. Ian Wilson<sup>2</sup>

<sup>1</sup>Department of Mathematics, University of Manchester, Manchester, M13 9PL, United Kingdom; email: julien.landel@manchester.ac.uk

<sup>2</sup>Department of Chemical Engineering and Biotechnology, University of Cambridge, Cambridge, CB3 0AS, United Kingdom

Xxxx. Xxx. Xxx. Xxx. YYYY. AA:1–26

[https://doi.org/10.1146/\(\(please add article doi\)\)](https://doi.org/10.1146/((please add article doi)))

Copyright © YYYY by Annual Reviews.  
All rights reserved

## Keywords

cleaning and decontamination, flow displacement, interfacial dynamics, mass transfer, multiphase flow, wetting

## Abstract

The removal of unwanted entities or soiling material from surfaces is an essential operation in many personal, industrial, societal and environmental applications. The use of liquid cleansers for cleaning and decontamination is ubiquitous and this review seeks to identify commonality in the fluid flow phenomena involved, and particularly those which determine the effectiveness of such operations. The state of quantitative understanding and modelling is reviewed in relation to the topics of (i) the cleanser contacting the soiled area; (ii) processes by which the cleanser effects soil removal; and (iii) transport of the soil or its derivatives away from the surface. The review focuses on rigid substrates and does not consider processes based on gas flows or bubbles.

## Contents

1. INTRODUCTION .....	2
1.1. Cleaning and decontamination scenarios considered .....	4
1.2. Surface tension forces and the three phase contact line .....	6
2. DISTRIBUTION OF THE CLEANSER AND CONTACTING THE SOIL .....	7
2.1. Flows in internal systems .....	7
2.2. Initial momentum driven flows .....	8
2.3. Gravity driven flows .....	10
2.4. Flows in porous media .....	11
3. ACTIONS OF THE CLEANSER ON THE SOIL .....	13
3.1. Mechanical action .....	13
3.2. Chemical action .....	14
3.3. Surfactant action .....	16
3.4. Temperature .....	16
4. TRANSPORT OF THE SOIL AWAY FROM THE SUBSTRATE .....	17
4.1. Advection processes .....	17
4.2. Diffusive processes .....	20
5. SUMMARY .....	21

## 1. INTRODUCTION

The cleaning of a surface involves the removal of an unwanted substance or ‘soil’ attached to the surface. Decontamination aims to achieve complete removal of such substances and frequently constitutes the final stage in a cleaning operation. Decontamination processes vary depending on the nature of the soil and whether it presents an immediate chemical, biological or radiological (CBR) hazard. In this review, we survey the literature describing how fluid mechanics determine the cleaning and decontamination (C&D) of surfaces by a liquid cleanser. We focus on soils in the form of liquids, soft solids and particles.



**Figure 1**

Illustrations of cleaning scenarios (from left) at home (manual, automated), in industry (cleaning a reactor), in the environment (simulation of water injection in porous media), and decontamination of personnel. [\[Permissions to request.\]](#)

Cleaning is ubiquitous in almost all human activities (see **Figure 1**) whether at home, in industry, in the natural environment or in public spaces. C&D is necessary for safety, for instance to maintain hygiene in a hospital or to avoid cross-contamination at product changeover in the pharmaceutical, cosmetic and food industries. It may be required for practical or business purposes, for instance to avoid the build up of soils which can lead to the damage, mal-function or failure of equipment. It may also be desired for aesthetic reasons in public and private spaces. Though often overlooked, or unwanted (who enjoys washing up?),

cleaning is nevertheless crucial to maintain a healthy and economically thriving society. Neglecting cleaning can have significant socio-economic consequences. Buildup of biological soils can become hazardous with much higher *decontamination* costs, whilst increasing the risks to health. Decontamination processes are also important for the specialised removal of toxic agents, for instance after accidental or terrorist releases, or the removal of radioactive material associated with nuclear activities or accidents.

Cleaning and decontamination are performed in many different contexts and scenarios, and feature various modes of action. The fundamental multidisciplinary physical and chemical processes underpinning cleaning problems are closely related when the cleaning agent takes the form of a liquid cleanser, whose action is governed by fluid mechanics. Such C&D operations involve multiphase flow dynamics across a wide range of spatial and time scales: from the decades-long cleaning of porous aquifers to the millisecond timescales involved in impinging liquid jets for high-pressure water jet cleaning; and from the sub-micron scale controlling contact line dynamics to the largest dimensions of the soiled surface. The framework of continuum mechanics and fluid mechanics can be used not only to study and understand these processes, but also to model and predict them. The phenomena involved, including multiphase flow, mass transfer, moving boundaries, interfacial dynamics, three-phase contact line dynamics, and many associated chemical and surfactant processes, have been investigated by fluid mechanicians for many decades. Although C&D is seldom stated as a direct application in fluid mechanics research, much progress on the underlying phenomena of the fluid mechanics of C&D has been made. This fundamental understanding can be harnessed to provide a more rigorous basis for the quantitative modelling and optimisation of a broad range of C&D operations, which have hitherto been performed empirically.

It is therefore surprising that no reviews have appeared on the fluid mechanics of cleaning and decontamination, particularly given the large and increasing amount of resources (clean water in particular) consumed in C&D activities. Previous reviews on the subject have focused on the technical and engineering aspects (Wilson 2005, Fryer & Asteriadou 2009). Many reviews and books about chemical aspects of cleaning exist: Rosen & Kunjappu (2012) (Chapter 10) focuses on the detergency effects of surfactants, Cutler & Kissa (1986) present a detailed description of chemical aspects of detergency, whilst Carroll (1993) focuses on some physical aspects of detergency. This review will present the central importance of fluid mechanics to many aspects of surface cleaning and decontamination processes, whilst connecting with research in engineering and chemistry. One of the aims of this review is to provide a starting point for readers interested in the quantitative modelling of specific cleaning and decontamination problems, with references providing more technical detail about specific points. We will also highlight challenges and unexplored aspects of this broad topic to guide future research effort.

The structure of the review highlights the role of fluid mechanics at each stage of C&D. The first stage, discussed in Section 2, is for the cleanser to contact the soil, which can present many challenges. The different modes of action by which the cleanser (and agents contained therein) removes a soil are considered in Section 3. Finally, Section 4 reviews the processes associated with transporting the soil away from the substrate. Each of these stages is necessary for the effective and timely removal of the soil regardless of the application.

## 1.1. Cleaning and decontamination scenarios considered

The general cleaning and decontamination scenarios considered in this review are represented schematically in **Figure 2**. Three phases are generally involved with internal flows, depicted in **Figure 2a–d**: a liquid cleanser, a soil (which may exhibit complex rheology) and a solid substrate on which the soil is located. A fourth phase may also be present, for instance ambient air in external flow problems, as depicted in **Figure 2e–g**. The scope of this review is restricted to problems where the cleanser is a liquid. The solid substrate remains rigid and fixed in time. This review will not cover C&D operations related to: particle resuspension in gases, *e.g.* vacuum cleaning; cavitation phenomena such as in ultrasonic cleaning; bulk fluid cleaning, *e.g.* waste water treatment and air scrubbing; cleaning by solids, *e.g.* scrubbing tools, erosion by particle impact (sand blasting, CO<sub>2</sub> blasting); foams and bubbles; and the cleaning of membranes used in separation processes.

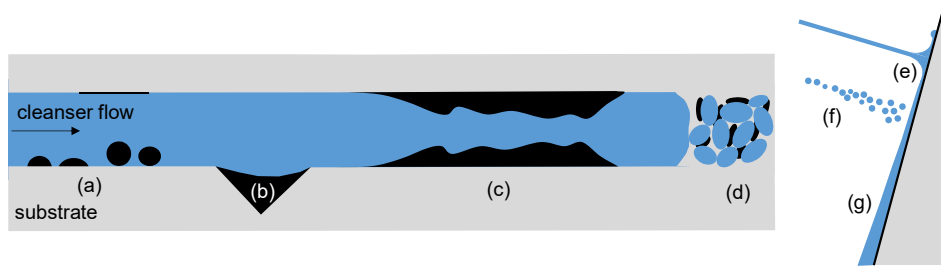


**Figure 2**

Schematic showing examples of cleaning and decontamination scenarios. A liquid cleanser (in blue) is used to remove a liquid, soft solid or particulate soil (in black) attached to a rigid solid substrate (in grey). Confined flows: (a) soiled duct wall; (b) soil in crevice; (c) purging and displacement; (d) porous matrix. Free surface flows: (e) impinging jet; (f) spray; (g) falling film.

The flow in the cleanser and in the soil (if mobile) must satisfy the conservation equations for mass and momentum, assuming an isothermal system (temperature effects are discussed in Section 3.4). The cleanser can be a mixture of chemical species, such as solvents, surfactants or detergents, reactive agents and particulate or dissolved soil. Similarly, the soil can be a mixture and often exhibits complex rheology. Conservation of mass in the cleanser and soil phases satisfies (Bird et al. 2002),

$$\frac{\partial \rho_i}{\partial t} = -(\nabla \cdot (\rho_i \mathbf{u})) - (\nabla \cdot \mathbf{J}_i) + R_i, \quad 1.$$

with  $\rho_i$  the mass concentration of species  $i$ ,  $t$  time,  $\mathbf{u} = \sum_i (\rho_i \mathbf{u}_i) / \rho$  the center-of-mass velocity of the mixture (bold symbols represent vectors),  $\mathbf{u}_i$  the local velocity of species  $i$  with respect to an inertial frame of reference,  $\mathbf{J}_i = \rho_i (\mathbf{u}_i - \mathbf{u})$  the diffusive mass flux of species  $i$ , and  $R_i$  the rate of production ( $R_i > 0$ ) or destruction ( $R_i < 0$ ) of mass of species  $i$  per unit volume by reaction. If a species  $i$  diffuses in the mixture following Fick's first law, the isotropic diffusive flux is  $\mathbf{J}_i = -D_i \nabla \rho_i$ , where  $D_i$  is the diffusivity of species  $i$  in the mixture. However, in more complex systems, such as for dense polymeric solutions or colloid solutions,  $\mathbf{J}_i$  may be more complex (Bird et al. 2002). Adding equations 1 for each species, and noting that  $\sum_i R_i = 0$ , the continuity equation for the mixture is

$$\frac{\partial \rho}{\partial t} = -(\nabla \cdot (\rho \mathbf{u})). \quad 2.$$

The conservation of momentum follows

$$\frac{\partial}{\partial t}(\rho \mathbf{u}) + \nabla \cdot (\rho \mathbf{u} \otimes \mathbf{u}) = \nabla \cdot \boldsymbol{\sigma} + \rho \mathbf{g}, \quad 3.$$

with  $\otimes$  the outer product,  $\boldsymbol{\sigma}$  the Cauchy stress tensor and  $\mathbf{g}$  gravity. We have assumed that gravity is the only body force, as is commonly the case in most C&D scenarios. The Cauchy stress tensor depends on the properties of the liquid mixture. For an incompressible isotropic Newtonian fluid, it reduces to  $\boldsymbol{\sigma} = -p\mathbf{I} + \mu(\nabla \mathbf{u} + (\nabla \mathbf{u})^\top)$ , with  $p$  the pressure,  $\mathbf{I}$  the identity tensor and  $\mu$  the dynamic viscosity of the mixture. Liquid cleansers are often assumed to be incompressible isotropic Newtonian fluids. Where the soil has a more complex rheology, see Section 4.1.1, a different constitutive equation relating  $\boldsymbol{\sigma}$  to  $\nabla \mathbf{u}$  may be needed. In the case where the soil takes the form of solid particles, only the cleanser is subject to the conservation equations above, and the interaction between the solid particles and the cleanser needs to be modelled (see Section 4.1.3).

The governing equations can have various boundary conditions. For non-porous and impermeable solid substrates, the no-flux  $\mathbf{u} \cdot \mathbf{n} = 0$  and no-slip  $\mathbf{u} \times \mathbf{n} = 0$  boundary conditions apply on solid surfaces, with  $\mathbf{n}$  the normal vector at solid surfaces. The boundary conditions between the cleanser and the soil determine the action of the cleanser on the soil. We can define the location of the interface by all the points satisfying  $S(\mathbf{x}, t) = 0$ , with  $\mathbf{x} = (x, y, z)$  the coordinates of a point in space. The velocity at the interface satisfies

$$\mathbf{v} \cdot \mathbf{n} = -\frac{1}{|\nabla S|} \frac{\partial S}{\partial t}, \quad 4.$$

with  $\mathbf{n} = \nabla S / |\nabla S|$ . For all points on the interface, the discontinuity across the interface in the density of a species  $i$  is (Prosperetti 1979)

$$[[\mathbf{J}_i]] \cdot \mathbf{n} + \left[ \left[ \frac{\rho_i}{\rho} \right] \right] \rho (\mathbf{u} - \mathbf{v}) \cdot \mathbf{n} = r_i, \quad 5.$$

with  $[[\zeta]]$  the jump of a quantity  $\zeta$  across the interface, such that  $[[\rho_i/\rho]]$  is the difference in the species concentration in mass ratio between the soil and the cleanser phase,  $r_i$  the rate of generation or destruction of species  $i$  per unit area due to chemical reactions at the interface. In the second term in Equation 5  $\rho$  and  $\mathbf{u}$  can be either the density and velocity of the cleanser mixture or of the soil mixture (Prosperetti 1979). Equation 5 assumes that the interface is a two-dimensional massless surface, which cannot accumulate mass. This assumption is in general valid, although in some cases molecules such as surfactant adsorb onto the interface (see Section 3.3). In practice, interfaces between miscible phases are not perfect two-dimensional surfaces with zero-thickness. We expect to find a sharp but continuous transition in the density field in the vicinity of the interface. Equation 5 should therefore be regarded as a modelling tool in the context of continuum mechanics. For immiscible fluids, Equation 5 reduces to the no-flux boundary condition  $(\mathbf{u} - \mathbf{v}) \cdot \mathbf{n} = 0$  on both sides of the interface, which is equivalent to the kinematic boundary condition  $\partial S / \partial t + \mathbf{u} \cdot \nabla S = 0$  on  $S = 0$ . The discontinuity in the momentum at the interface is

$$[[\boldsymbol{\sigma}]] \cdot \mathbf{n} = \gamma (\nabla \cdot \mathbf{n}) \mathbf{n} + \nabla_s \gamma, \quad 6.$$

with  $\gamma$  the cleanser–soil surface tension,  $(\nabla \cdot \mathbf{n})$  the curvature of the interface, and  $\nabla_s = \nabla - \mathbf{n}(\mathbf{n} \cdot \nabla)$  the surface gradient operator. Other boundary conditions may be necessary to

ensure the problem is well posed. If viscosity effects are important in both phases, continuity of the tangential components of the velocity is imposed at the interface (Prosperetti 1979),

$$[[\mathbf{u}]] \times \mathbf{n} = 0. \quad 7.$$

For species diffusing across the interface, we also require at the interface,

$$\rho_i^{\text{cleanser}} = \kappa \rho_i^{\text{soil}}, \quad 8.$$

where superscripts designate the phase, and  $\kappa$  is a partition coefficient between the cleanser and the soil. This condition assumes that the interface is instantaneously at thermodynamic equilibrium. We note that the boundary conditions 5–8 all apply at the interface, whose position may change with time. Hence, most C&D scenarios also require the solution of moving boundary problems, where the unknown interfacial velocity  $\mathbf{v}$  (see Equation 4) needs to be determined simultaneously. At impermeable solid surfaces (assumed fixed here), no-diffusive flux is imposed,  $\partial \rho_i / \partial \mathbf{n} = 0$ . At other boundaries, including boundaries at infinity for open systems: a Dirichlet,  $\rho_i = c$ , Neumann,  $\partial \rho_i / \partial \mathbf{n} = c$ , or Robin,  $a \rho_i + b \partial \rho_i / \partial \mathbf{n} = b$  (with  $a$ ,  $b$  and  $c$  constants) boundary condition must be imposed depending on the scenario. Appropriate boundary conditions should also be imposed for the flow field at non-solid surfaces or infinity.

Note that various definitions exist for the *cleaning* and *decontamination rates*. Dimensional and non-dimensional fluxes (amount of soil per unit area per unit time) are used, as are measures of the rate at which a soil-free surface is generated, depending on the context.

## 1.2. Surface tension forces and the three phase contact line

The forces that bind a soil to itself (cohesion) and to a substrate (adhesion) have been reviewed elsewhere (e.g. Israelachvili (2011)) and are fundamental to understanding soil behaviour and the selection of cleaning agents. Differences in cohesion between phases determine wetting behaviour and surface tension forces.

Surface tension forces determine the geometry and dynamics of three-phase contact lines, which are central to cleaning and decontamination. These are termed *contact lines* hereafter. C&D applications have a contact line between the cleanser, the soil and the substrate. Another contact line may be present between the cleanser, the atmosphere and the substrate, demarking a wetted region from a dry or a recently wetted region. For continuum analyses, Young’s relation describes the static force balance at the contact line (Dussan V. 1979). Contact line hysteresis  $\theta_a - \theta_r$  (with  $\theta_a$  and  $\theta_r$  the advancing and receding contact angles, respectively, **Figure 3a**) and contact line pinning are important phenomena, which have a strong influence on the motion of the cleanser over the substrate (Thampi et al. 2016). These phenomena also control the mobility of a liquid or soft solid soil on the substrate.

Moving contact lines are challenging to model in continuum analyses, owing to the dynamic singularity found at the contact line (Snoeijer & Andreotti 2013). The difficulty is to reconcile the no-slip boundary condition at the substrate with the motion of the liquid phases (**Figure 3b**). Many models have been proposed to regularise this singularity, such as introducing a Navier-slip length, modelling molecular interactions through a disjoining pressure, or via diffuse interface models (Snoeijer & Andreotti 2013). Sui et al. (2014) give a useful recent review of numerical methods modelling the moving contact line, such as the level-set, volume of fluid, front-tracking and diffuse interface methods. Molecular dynamics

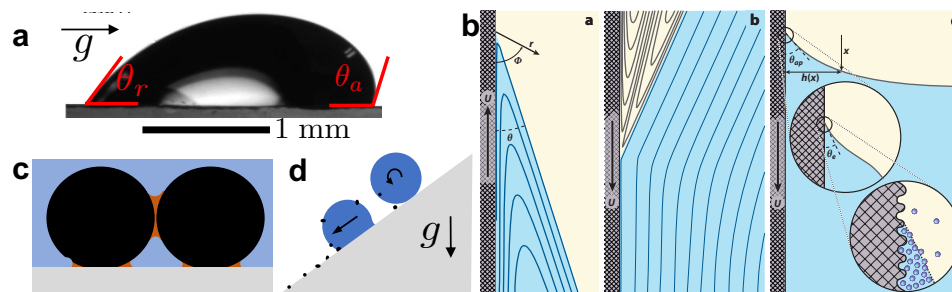


**Figure 3**

(a) Sessile drop on a vertical substrate showing the advancing and receding contact angles. Adapted with permissions from Kim et al. (2017) [To request]. (b) Schematic showing a (i) receding, and (ii) advancing three-phase contact line, which arises in many cleaning and decontamination scenarios; (iii) illustrates the distinction between apparent ( $\theta_{ap}$ ) and true ( $\theta_e$ ) contact angle at the macroscopic and nanoscopic scales, respectively. Adapted with permissions from (Snoeijer & Andreotti 2013) and Bonn et al. (2009) [To request; also change a, b and c to (i), (ii) and (iii)]. Examples of three phase contact lines in particulate removal: (c) wetting liquid (orange) immiscible in cleanser (blue) creates liquid bridges from particles (black) to substrate (grey); (d) sliding or rolling liquid droplets pick up particulates from dry substrate.

simulations (Smith et al. 2018) are now able to link continuum understanding to molecular scale behaviour. However, there are still difficulties in capturing contact angle hysteresis accurately due to the multiphysics and multiscale nature of the problem (Sui et al. 2014).

Choosing the contact angle of a soil is challenging, as they often have heterogeneous composition and uneven morphology, thus combining Cassie–Baxter and Wenzel behaviour. The design of functional and biomimetic surfaces has prompted extensive work in this area (Sethi & Manik 2018). The challenge is how to transfer that understanding to real soils.

## 2. DISTRIBUTION OF THE CLEANSER AND CONTACTING THE SOIL

The first stage of any C&D process is for the cleanser to reach the soil. How the cleanser is applied will influence the distribution of the cleanser over the soiled area, and the removal mechanism. Depending on the application, there may be a choice of delivery mode, allowing optimisation to reduce cleanser and chemicals consumption, energy and cleaning time. There are also many scenarios where geometrical, physical or chemical constraints dictate a particular mode of delivery. In particular, confined spaces (porous materials, narrow gaps) and/or inaccessible regions (e.g. piping networks in factories, internal surfaces of process equipment) dictate the mode of delivery. Understanding the processes involved can improve C&D performance.

### 2.1. Flows in internal systems

Numerous industrial processes require the cleaning or decontamination of internal surfaces of equipment, pipes and channels (**Figure 2a–c**). C&D of internal surfaces can be challenging as accessing soiled surfaces may be difficult. The physical dismantling of the system may be technically unfeasible, costly, or create undesirable exposure (whether release of contents to the atmosphere or microbial contamination from the surroundings). Regular cleaning

of manufacturing lines is performed in the food, pharmaceutical and consumer goods (*e.g.* cosmetics) industries by automated Cleaning-in-Place (CIP) systems. Liquid cleansers, driven by pressure gradients or gravity, are normally employed to reach and remove soils in such systems. As we will discuss in Section 3, liquid cleansers can perform cleaning action by themselves in a number of ways, or act as a carrier for a cleaning agent.

There are nevertheless challenges associated with the effective use of liquid cleansers in internal systems. For complex internal geometries, the cleanser may not be able to reach every soiled part of the system. Corners, cavities, narrow gaps or close-ended side channels can trap air bubbles when the characteristic size of these features is less than the capillary length  $\lambda_c = \sqrt{\gamma/(\Delta\rho g)}$ , with  $\Delta\rho$  the density difference between the cleanser and the air.

Even when the system is flooded and no air bubbles remain, flow separation can occur (Higdon 1985). Different regions can be completely separated, *e.g.* a deep crevice (**Figure 2b**), such that there is no advection across the boundary. In such ‘dead zones’ only diffusive processes are active, following the same boundary condition, Equation 5, as for an interface between two phases. Hence, the cleaning rate in these regions, typically found upstream or downstream of sharp corners, can be significantly hampered (Fang 2003). They can exist at low Reynolds numbers,  $\mathcal{R}e = UL/\nu \ll 1$  (with  $U$  a characteristic velocity of the flow,  $L$  a characteristic length and  $\nu = \mu/\rho$  the kinematic viscosity of the cleanser) and the shape of the separatrix is sensitive to geometry (Higdon 1985). The flow inside shows recirculation patterns, such as Moffatt eddies in corners (Moffatt 1964) or a stack of eddies in shear- or lid-driven cavity flows (Shankar & Deshpande 2000). The eddy strength decreases rapidly away from the separatrix, thus reducing the mechanical forces of the cleanser.

Destabilising the separatrix can improve the cleaning rate of soiled surfaces in separated regions. At  $\mathcal{R}e \gg 1$ , flow instabilities such as the Kelvin–Helmholtz or centrifugal Taylor–Görtler-like instabilities can destabilise the separatrix (Douay et al. 2013). They induce flow injection and ejections in and out of the separated region, enhancing the mass transfer and cleaning rate (Chang et al. 2018). The main drawback is the increase in energy consumption.

Destabilising the separatrix through high Reynolds number flow instabilities may not always be achievable. Nevertheless, at lower  $\mathcal{R}e$ , the separatrix can still be disrupted by inducing spatial or temporal disturbances in the flow, *e.g.* pulsing (Horner et al. 2002). The disruption of the separatrix depends on  $\mathcal{R}e$ , the Womersley number (ratio of transient inertia in pulsed flows to viscous forces), and the geometry. It manifests in flow ejections, in and out of the cavity, through a complex chaotic entanglement of the separatrix (Horner et al. 2002). Promoting chaotic advection at the interface and in the cavity can enhance mass transfer, and thus cleaning rate, by up to 3 orders of magnitude compared with steady flows (Nishimura & Kunitsugu 1997, Horner et al. 2002).

## 2.2. Initial momentum driven flows

**2.2.1. Jet impingement.** Liquid jets can be used both to deliver cleanser to a surface and to effect removal (**Figures 2e** and **4**). The liquid flows on the substrate as a thin liquid film moving radially away from the point of impingement until a jump (abrupt change in thickness) occurs, where the characteristic time scales and velocities change noticeably. The shape of the region bounded by the jump depends on the angle of impingement and gravity (Bhagat & Wilson 2016): on an inclined wall the lower part of the radial film may become a falling film without forming a jump. There is ongoing debate over the role of

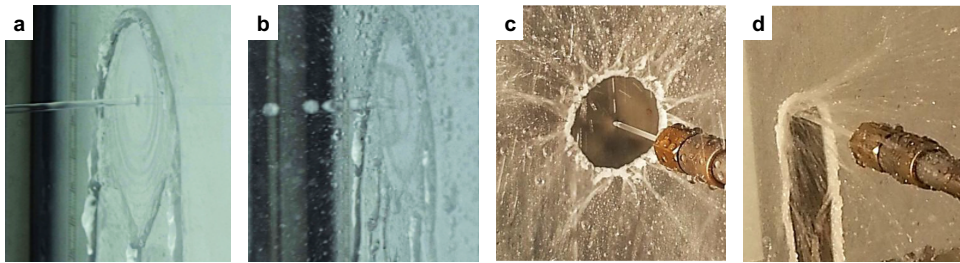


**Figure 4**

Illustration of a horizontal water jet of diameter  $d_N$  and length  $L$  impinging on a soiled vertical substrate showing (a) a coherent jet ( $L/d_N = 90$ ), (b) jet breakup in flight ( $L/d_N = 260$ ) causing extensive splashing ( $Re = 10,600$ ,  $We = 760$ , with  $Re = d_N U/\nu$  the jet Reynolds number and  $We = \rho d_N U^2/\gamma$  the jet Weber number); and removal of the soil (petroleum jelly) by (c) a static jet and (d) a moving jet. Photographs courtesy of MWL Chee (a,b) and RK Bhagat (c,d).

surface tension and gravity in determining the location of the hydraulic jump,  $R_j$ , formed by coherent jets: Bhagat et al. (2018) derived a scaling of the form  $R_j = (Q^3 \rho/(\nu\gamma))^{1/4}$  (with  $Q$  the volumetric flow rate) for turbulent water jets, which holds for vertical and inclined walls, and for jumps formed by jets from moving nozzles.

The jump separates the area contacted by the jet into two regions relevant to cleaning: (i) the radial flow zone, near the impinging point, characterised by short time scales and high velocities, and (ii) the thick film region, where gravity has greater influence on the film flow. For jets impinging on the underside of a horizontal plate, region (ii) takes the form of a water bell or curtain of falling droplets (Jameson et al. 2010), while jets impinging obliquely on superhydrophobic surfaces can exhibit detachment rather than spreading (Kibar et al. 2010). On an inclined substrate, the thick film spreads outwards and eventually changes to a falling film bounded by ropes (**Figure 5a**, Section 2.3) with the extent of the wetted area dictated by the balance between outward momentum and surface tension acting at the contact line (Aouad et al. 2016). It should be noted that in cleaning applications the contact angle can vary over time as a result of soil removal and changes in surface morphology.

Capillary and gravity waves are often observed in both regions (**Figures 4a** and **5**), as well as waves induced by fluctuations in the liquid supply rate or pressure. These influence the local momentum, mass and heat transfer rates, and thus the cleaning rate (Craster & Matar 2009).

Surface tension and drag from the surrounding gas can cause jets to lose coherence (**Figure 4b**), *e.g.* via the Rayleigh–Plateau instability, promoting break-up and droplet formation (Theofanous 2011). Lin & Reitz (1998) review the regimes observed with cylindrical liquid jets. Trains of droplets generated by incoherent jets produce jumps and falling films, as above, with wave and pressure periodicity set by the droplet frequency. Mitchell et al. (2019) investigated the normal force generated by a coherent jet and a train of droplets created by subjecting the same jet to an external excitation. Their model gave good agreement with the measured increase in impulse generated by the droplet train. Droplets arriving on a wetted surface cause splashing and side jetting (**Figure 4b**; Kondo & Ando 2019), reducing the flow rate in the radial film and liquid film downstream (Chee et al. 2019).

Jet break-up is influenced by nozzle geometry and increases with distance travelled. It is one of the main challenges in scaling up results from laboratory experiments to application

length scales. A range of nozzle shapes is used in practice, including slots to generate liquid sheets: many of these are employed to promote wetting of the substrate and to generate a falling film, rather than a fast moving thin film near the impinging point.

A second challenge in modelling jet cleaning is that the cleanser is often delivered by one or more moving nozzles, *e.g.* generated by rotating jet heads, so that the point of impingement traverses a surface which is already wetted by a falling film. The radial film zone persists but the jump and falling films can be quite irregular. With non-wetting soils, different dynamics can arise and falling films may not exist (**Figure 4c–d**).

**2.2.2. Sprays.** Jets and sheets can be broken intentionally to form sprays or trains of droplets with different cleaning properties to those of coherent jets (**Figure 2f**). Lin & Reitz (1998) reviewed the break-up dynamics, instabilities and droplet fragmentation and dispersion in a gas. The velocity of the liquid through the nozzle and the nozzle design determine the form of the spray. Large spray angles and low velocities promote air entrainment and the formation of a wetting mist, while high velocities and narrow angles generate droplet trains suitable for decoating (Mabrouki et al. 2000) and water-jet cutting (Li et al. 2017).

The velocity of a single drop in quiescent air is quantified by the Stokes number, but the entrainment of ambient air in a spray or droplet train gives rise to coupled two-phase problems which require numerical solution (Gorokhovski & Herrmann 2008).

Once on the surface, the shape of a static or slow moving drop is determined by the balance between gravity and surface tension, expressed in the Bond or Eötvös number ( $\mathcal{E}o = \Delta\rho g d^2 / \gamma$ , with  $\Delta\rho$  the liquid–air density difference and  $d$  the drop diameter), with large drops tending to be non-spherical. Drops can coalesce to form films (Section 2.3) or rivulets, which may flow further following a force balance between gravity, wetting (surface tension and contact angle) and viscosity (Perazzo & Gratton 2004). Sprays employ smaller quantities of liquid than jets to contact a given area of substrate, but limits the mechanical action to that of drop impingement and shear of a falling film or rivulet (see Section 3.1).

The spreading of a drop on a wetting surface is driven by surface tension (and reduction in contact angle), working against viscosity. The shape of drops of non-Newtonian fluids and their spreading has been studied at length in connection with inkjet applications (Jung & Hutchings 2012). On an inclined non-wetting surface droplets may roll and collect particulate matter from the substrate surface (**Figure 3d**). Combining sprays with suitably structured surfaces has been investigated to clean solar cells (Hassan et al. 2019).

### 2.3. Gravity driven flows

Falling liquid films can be generated by jets and sprays, weirs and slots, or flows on the inner and outer surfaces of pipes. They can be used to access locations at lower heights which are inaccessible by direct delivery, and which are not suitable for internal flows, or for surfaces which cannot be readily immersed. There is a large body of literature on the dynamics, heat and mass transfer in falling films owing to their role in devices such as falling film evaporators, on understanding and modelling instabilities at the surface using long-wave asymptotic and thin film approximations (Chang 1994, Craster & Matar 2009), the flow inside the film (*e.g.* viscous–gravity driven, lubrication approximation), and surface tension effects near the contact line.

The film can spread across a surface or retract to form dry patches and rivulets, de-

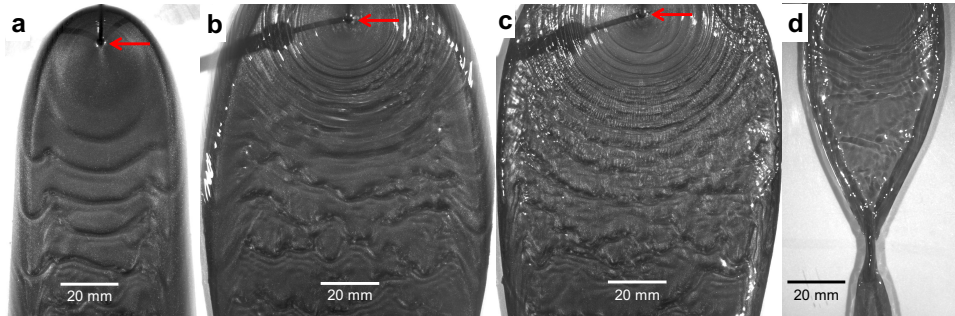


**Figure 5**

Illustration of a falling film produced by a normally impinging jet (red arrow) for soil displacement on a vertical substrate. As the jet Reynolds number increases: (a)  $Re = 1100$ , (b)  $Re = 2600$ , (c)  $Re = 4800$ ; the draining film flow displays a variety of interfacial instabilities (Craiser & Matar 2009). (d) The film braiding pattern is due to wetting and dewetting phenomena at the substrate. [Permissions or approval needed]

pending on the surface properties (geometrical and chemical). Rivulets can exhibit braiding patterns (Mertens et al. 2005). None of these are desirable from a cleaning perspective. Dewetting occurs when the local momentum flow rate is weaker than the surface tension force acting at the resulting contact line. Predicting dewetting — identifying critical flow rates per unit length — builds on results such as Hartley & Murgatroyd (1964)'s  $m_L = 1.69(\mu\rho/g)^{1/5}(\gamma(1 - \cos\theta))^{3/5}$ , with  $m_L$  the mass flow rate per unit length and  $\theta$  the contact angle on an ideal substrate. Waves can cause the dewetting front to fluctuate and move, introducing further dynamics. When surfactants are present, the flow can be subject to Marangoni and diffusion effects (Section 3.3).

## 2.4. Flows in porous media

One of the most important C&D operations in porous media is groundwater remediation (Kahler & Kabala 2016). Water-miscible contaminants disperse slowly in the aquifer, invading areas of low permeability which renders their removal challenging (NRC 1994). Immiscible contaminants present removal challenges analogous to the multiphase displacement of oil in enhanced oil recovery (EOR) (Payatakes 1982). Some contaminants can be absorbed or adsorbed in the porous solid matrix. Their slow desorption is also challenging.

Pump-and-treat (P&T) is a common remediation method consisting of pumping out contaminant-rich water, and treating it before reinjection in the aquifer (Kahler & Kabala 2016). However, P&T is expensive and lengthy with costs  $\sim$ \$1 trillion in the US and cleaning operations lasting over decades (NRC 1994).

At the pore-scale, porous media flows depend on pore geometry and multiphase interactions at fluid–fluid interfaces and contact lines. Owing to the technical difficulties in modelling the flow at the pore-scale, macroscale models are used to estimate the average flow. In a homogeneous isotropic porous medium, a multiphase flow with immiscible phases typically follows Darcy's law (Wooding & Morel-Seytoux 1976),  $\mathbf{u}_i = -K K_{r,i} / \mu_i (\nabla p_i - \rho_i \mathbf{g})$  for phase  $i$ , with  $K$  the empirical intrinsic permeability of the medium and  $K_{r,i}$  the em-

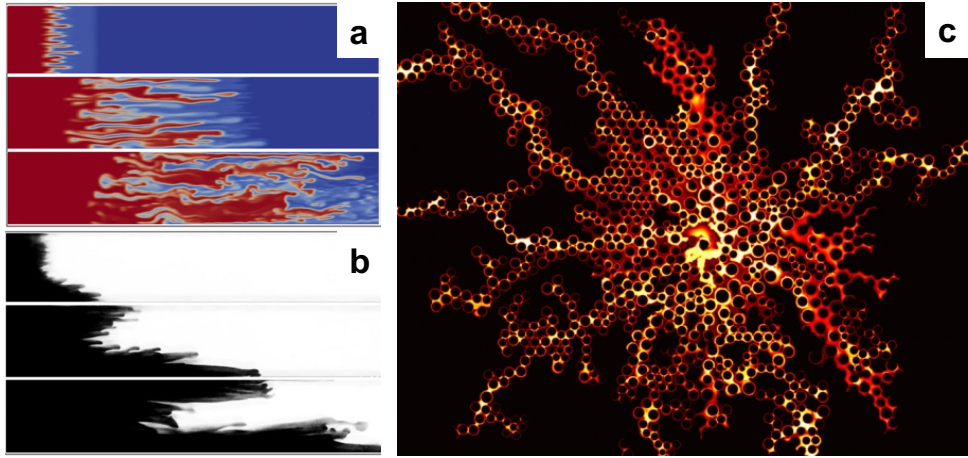


**Figure 6**

Illustrations of multiphase flow displacement in porous media. Saffman–Taylor instability with viscoelastic–Newtonian immiscible fluid displacement in a Hele–Shaw cell: (a) numerical simulation, (b) experiments. Adapted with permissions from (a) Yazdi & Norouzi (2018) and (b) Vaezi (2015) [To request]. (c) Displacement pattern in porous media; experiments in a microfluidic cell with vertical posts, testing the impact of wettability and viscosity on the invasion at pore-scale. Adapted with permissions from Zhao et al. (2016) [To request].

pirical relative permeability of phase  $i$ . The pressure gradient  $\nabla p_i$  can be due to external pumping or capillary pressure (Wooding & Morel-Seytoux 1976). The mass conservation statement, Equation 1, is written as  $\phi \partial s_i / \partial t = -\nabla \cdot \mathbf{u}_i$ , with  $\phi$  the medium porosity, and  $s_i$  the saturation (volume of phase  $i$  per unit volume of voids). In addition, thermodynamic equations of state are needed to relate pressure and saturation in each phase.

The validity of the macroscale equations is still debated. Experiments have shown hysteresis behaviour in wetting and dewetting cycles. The homogeneous and isotropic assumptions are questioned as realistic porous media are heterogeneous and potentially anisotropic. The effect of vapour diffusion and air pressure can also be important (Wooding & Morel-Seytoux 1976). With the recent increase in computational power, numerical simulation of the microscale equations is possible, though contact line dynamics remains challenging.

Poorly connected pores or low permeability regions can store large quantities of contaminant, which cannot be reached by advection but only by transverse diffusion, reducing the efficiency of continuous P&T. Instead, intermittent P&T improves the cleaning efficiency (in terms of mass of contaminant removed per volume of water pumped) as it allows contaminant to diffuse out of poorly connected pores or desorb from the matrix (Mackay et al. 2000). However, the overall cleaning time is longer than with continuous P&T.

Contaminant trapped in dead-end pores are separated from the main flow by a separatrix. Similar to the separatrix disruption methods discussed in Section 2.1, Kahler & Kabala (2016) proposed rapid unsteady pumping to clean dead-end pores more effectively in aquifer remediation. Their numerical and experimental results showed clear enhancement of mass transfer and overall contaminant recovery. However, rapid unsteady pumping is only effective for miscible contaminants which are not absorbed into the porous matrix.

Contaminants in porous media can also be removed through flow displacement (Pay-

atakes 1982) (see Section 4.1.1). However, the displacement of a more viscous contaminant by a less viscous cleanser can lead to the Saffman–Taylor instability (Homsy 1987), preventing full displacement of the contaminant (**Figure 6a,b**). This instability has been studied in Hele–Shaw flow cells which provide a simple flow setup governed by analogous equations.

### 3. ACTIONS OF THE CLEANSER ON THE SOIL

#### 3.1. Mechanical action

Cleaning and decontamination through mechanical action is commonly used for internal and external surfaces, as well as porous media. As shown in **Figure 2**, stresses generated by the cleanser flow can detach or displace soils by overcoming adhesion and cohesion. The mechanical action is the result of all the forces exerted by the cleanser onto the soil, which can be determined by solving the governing equations presented in Section 1.1.

Computing the mechanical action can be challenging as it requires solving a coupled, nonlinear, multiphase flow problem governed by partial differential equations. For complex geometries, numerical simulations are often the only way to compute the mechanical action and the displacement of the soil. The problem usually depends on time because the soil deforms or moves, or the flow of cleanser varies over time. The boundary condition at the soil–substrate interface is crucial as it models the soil–substrate adhesion. A no–slip boundary condition is often used, as considered here. However, this boundary condition is problematic as it does not allow the soil to move at the substrate. The onset of motion and the contact line dynamics must therefore be modelled carefully, as discussed in Section 1.2.

The cohesion forces within the soil are modelled through its rheology. Complex soil rheology can introduce nonlinearities in Equation 3, making resolution more challenging (Bird & Wiest 1995, Balmforth et al. 2014). For soils without a yield stress, flow within the soil starts as soon as the external forces applied at the interface depart from static equilibrium. If the soil has a non-zero yield-stress, determining the location of the yield surface is critical (Balmforth et al. 2014). Many soils in practice exhibit complex, time-dependent rheology where phenomena such as creep would have to be modelled in order to capture all the observed features faithfully. Reduced order models can nevertheless give useful results for understanding and improving C&D methods, within feasible timescales.

Many C&D scenarios involving mechanical action have been studied. We review below a few examples where mechanical action from the cleanser is the primary mode of cleaning.

Impinging jets and sprays are often used for the C&D of external surfaces. However, determining the mechanical action at the point of impact is challenging as this can include ballistic effects such as water hammer (Tatekura et al. 2018) as well as gouging (Chen & Bertola 2017). Yeckel et al. (1994) studied the distribution of shear and pressure in the stagnation region of a coherent jet and the flow in a thin film of mobile soil in the radial flow zone. Their model, based on the lubrication equations, showed good agreement with experiments on the displacement of a viscous film of an immiscible Newtonian oil on a flat substrate by a turbulent water jet. The removal of non-Newtonian soils by impinging jets has been investigated for viscoelastic soils (Hsu et al. 2011) and shear-thinning soils (Walker et al. 2012). These studies showed how the developing Saffman–Taylor instability and the perturbation of the film jump can modify the shear and pressure distribution on the soil, affecting its removal.

The depth of the crater created by impinging spray drops and broken jets has received much attention. For single drop impact, which is relevant to spray cleaning (Guha et al.

2011), splashing occurs if  $WeOh^{-2/5} > 2100 + 5880H^{1.44}$ , with  $We = \rho dV_0^2/\gamma$  the drop Weber number,  $Oh = \mu/(\rho\gamma d)^{1/2}$  the Ohnesorge number,  $H = h_0/d$  the dimensionless film thickness, and  $V_0$  the impact velocity (Yarin 2006). If a train of drops or a coherent liquid jet impinge on a liquid soil, the depth of the cavity increases depending on the frequency of drop impact, the Bond number and the Weber number, and the depth of the soil layer.

**Figure 4c,d** shows a liquid jet removing a viscoplastic soil layer. The jet has sufficient inertia to penetrate the soil and form a circular crater which grows over time, removing soil through displacement. The immiscible soil collects as a berm at the cleaning front. Reduced order models have been developed for both static and moving jets, *e.g.* (Glover et al. 2016): the challenge here is to develop rigorous models based on Equations 1–6.

Flow pulsing and cavitation can enhance cleaning capabilities of impinging jets (Zohourkari et al. 2014). A resonator in the jet nozzle can induce large scale ring vortices in unstable axisymmetric jets. When excited at the correct frequency, the jet instabilities can produce large pressure oscillations, whilst the vortices can cavitate leading to water hammer effects. Li et al. (2017) showed that pressure oscillations and cavitation can be produced simultaneously in self-resonating water jets generated using an organ-pipe nozzle. This combined effect enhances the erosion and abrasion capabilities of these jets.

## 3.2. Chemical action

An agent is often introduced to change the soil so that it can be cleaned more readily, either by reducing the adhesion to the substrate (promoting lift-off or peeling), breaking a layer into mobile elements, or changing its rheology. The flow determines the rate of transport of this weakening agent as well as the hydraulic forces imposed on the soil. It must be noted that decontamination or sterilisation applications may not require removal of the soil from the substrate, where the primary aim is to neutralise a component, *e.g.* a chemical and biological warfare entity. More than one agent may be required: for instance with biofilms, one to kill the organism and others to promote detachment of the dead cells and residual material such as EPS (extracellular polymeric substances, secreted by cells to promote adhesion) in order to inhibit recolonisation of the surface (Melo & Bott 1997).

**3.2.1. Dissolution.** The simplest case of chemical action is to change the environment (temperature, pH, composition) so that the soil, or part thereof, dissolves. Erosion of the surface is often controlled by diffusion, either of the agent towards the soil or the mobilised soil into the fluid, or of the thermal energy required to effect the phase change. If a heterogeneous soil contains a soluble phase, dissolution will increase the volume fraction of cleanser and reduce the cohesive strength of the material, promoting erosion by mechanical action. The boundary condition at the dissolution interface often follows continuity of mass flux: Equation 5, and a Dirichlet interfacial condition for the concentration; Equation 8.

Dissolution of polymers is more complex as this involves several composition-dependent phases, with noticeable differences in rheology (Miller-Chou & Koenig 2003). Cleaning polymer layers (*e.g.* photoresists, Hunek & Cussler 2002) requires quantification of the rate of conversion between each phase and removal, by advection-enhanced diffusion, of the dilute phase.

**3.2.2. Swelling of soil.** A chemically compatible cleanser can absorb into the soil and cause it to swell (or shrink), modifying its intrinsic rheological and chemical properties, and

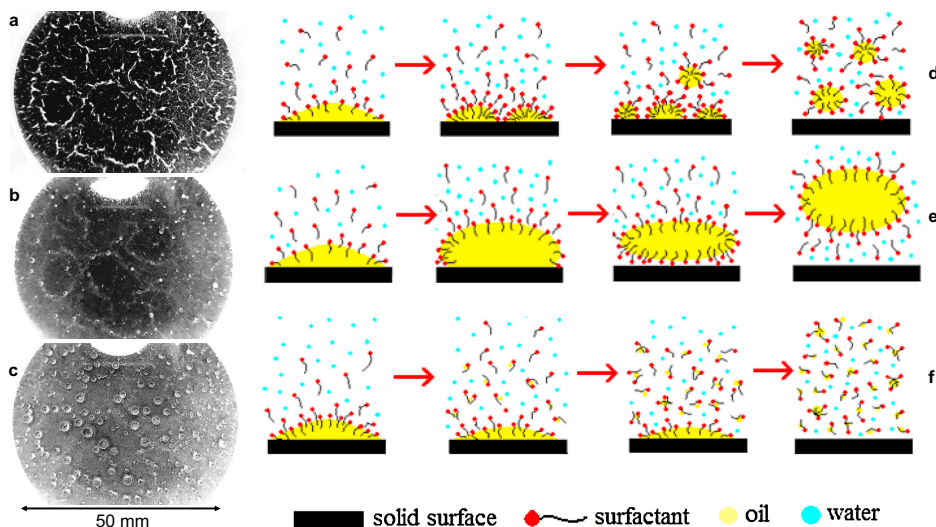


**Figure 7**

Left, contact of surfactant-rich liquid cleanser with cracked (baked) food soil (*a*) promotes swelling of matrix, closing cracks (*b*). Ingress of surfactant releases oil phase from the soil matrix to form droplets on its surface (*c*). Images provided by GL Cuckston. Right, surfactant effects on oily soil attached to a solid substrate immersed in aqueous surfactant cleanser: (*d*) emulsification of soil; (*e*) increase of soil contact angle  $\theta$  leading to soil detachment by buoyancy or mechanical action; (*f*) solubilisation of soil. Adapted with permissions from Wang et al. (2015) [To request].

changing its spatial structure. Swelling introduces diffusion and reaction timescales in the problem and the soil properties. **Figure 7** shows an example of a food soil where swelling on contact with cleanser closes up the cracks in the macrostructure and is followed by slow release of an oil phase present in the soil.

Swelling (and shrinking) of polymers and biopolymers in aqueous solution can be driven by changes in local pH and ionic strength. It can exhibit a two-step process whereby rapid initial hydration (absorption of solvent promoting relaxation of chains) is followed by chemistry-induced swelling (Schott 1992). The latter can be diffusion or diffusion–reaction controlled: detailed modelling of swelling has been driven by interest in photoresists (Tsiartas et al. 1997), hydrogels (Bouklas et al. 2012) and related materials employed in controlled release products. When a polymer is present within a porous matrix, the initial swelling dynamics is often governed by capillarity, with the pore size changing as a result of swelling (Markl et al. 2017).

When swelling promotes erosion of the swollen soil, cleaning features two moving fronts: one tracking the penetration of the species promoting swelling into the unswollen material, and the other the interface with the cleanser phase. A range of solutions can exist, depending on the rate of transport of agent through the soil, the swelling behaviour, and the rate of removal of swollen material. For example, proteinaceous dairy fouling deposits are removed by contact with alkali, which promotes swelling and breakdown of whey proteins. The cleaning rate exhibits a steady state corresponding to the penetration rate matching the erosion of the swollen deposit (Xin et al. 2004).

### 3.3. Surfactant action

If surfactants are present, they can adsorb at the soil surface, altering the surface tension, with extent governed by thermodynamics, through a constitutive law such as

$$\gamma = \gamma_0 + 2\mathcal{R}T\Gamma_m \left[ \ln \left( 1 - \frac{\Gamma}{\Gamma_m} \right) - \frac{A}{2} \left( \frac{\Gamma}{\Gamma_m} \right)^2 \right], \quad 9.$$

with  $\gamma_0$  the surfactant-free cleanser–soil surface tension,  $\mathcal{R}$  the universal gas constant,  $T$  temperature,  $\Gamma_m$  the maximum packing concentration of surfactant at the interface and  $A$  the Frumkin interaction parameter (Prosser & Franses 2001). The mass conservation of surfactant, or other species, at the interface is

$$\llbracket \mathbf{J}_i \rrbracket \cdot \mathbf{n} + \left[ \left[ \frac{\rho_i}{\rho} \right] \right] \rho (\mathbf{u} - \mathbf{v}) \cdot \mathbf{n} = - \left( \frac{\partial \Gamma_i}{\partial t} + \mathbf{v}_s \cdot \nabla_s \Gamma_i \right) - \Gamma_i (\mathbf{v} \cdot \mathbf{n} (\nabla \cdot \mathbf{n}) + \nabla_s \cdot \mathbf{v}_s) - \nabla_s \cdot \mathbf{j}_i + r_i, \quad 10.$$

with  $\Gamma_i$  the mass concentration (per unit area) of species  $i$ ,  $\mathbf{v}_s = \mathbf{v} - \mathbf{n}(\mathbf{n} \cdot \mathbf{v})$  is the tangential velocity at the interface, and  $\mathbf{j}_i$  represents non-convective fluxes of species  $i$  along the interface (Prosperetti 1979). Non-convective fluxes are typically diffusive fluxes which may be modelled using a two-dimensional Fick's first law  $\mathbf{j}_i = -D_{s,i} \nabla \Gamma_i$ , with  $D_{s,i}$  the surface diffusivity of species  $i$ . For soluble surfactant, the absorption and desorption fluxes of surfactant are captured by  $\llbracket \mathbf{J}_i \rrbracket \cdot \mathbf{n}$ . Various kinetic models describe the adsorption and desorption fluxes, depending on the type of surfactant (Prosser & Franses 2001).

The impact of surfactant on the detergency of cleansers has been discussed extensively (*e.g.* Rosen & Kunjappu 2012). It depends on the type of surfactant, soil, substrate and cleanser. The main effect of surfactant is to modify the adhesion forces binding a soil to a substrate. An effective surfactant changes the surface tensions, following Equation 9, so that the contact angle between the soil and the substrate increases. This is known as the roll-up or roll-back mechanism (**Figure 7e**). If the contact angle  $\theta$  approaches  $180^\circ$ , the soil can spontaneously detach from the substrate. For  $90^\circ < \theta < 180^\circ$ , the soil may detach fully under mechanical action from the flow. For  $\theta < 90^\circ$ , mechanical action may not fully remove the soil from the substrate.

Oily soils can be solubilised (**Figure 7f**) in aqueous cleansers by surfactant if the surfactant concentration is higher than the critical micellar concentration (CMC). The rate of solubilisation typically increases with the surfactant concentration and the oil polarity, and decreases with the oil molecular weight (Carroll 1981). Above the CMC, surfactant can promote the emulsification of the soil, and prevent re-deposition (**Figure 7d**).

Marangoni stresses in the dynamic boundary condition, Equation 6 (last term), can arise from surfactant concentration gradients at the interface. Marangoni stresses can play a role in the emulsification of oily soils (Rosen & Kunjappu 2012).

### 3.4. Temperature

Many fluid properties relevant to C&D depend on the local temperature, as are the behaviour and properties of the soil. For instance, temperature can modify the density, rheology (*e.g.* viscosity), diffusivity, surface tension, and partition coefficients. Constitutive equations modelling the temperature dependence of all these quantities should be added to the governing equations presented in Section 1.1. A governing equation for the conservation of heat, coupled with the other governing equations, should be solved simultaneously, under appropriate boundary conditions.

The chemical equilibria determining dissolution are temperature dependent, as are phase changes such as melting or softening wherein a solid soil becomes mobile under the imposed stress field. An example of this is the roll-up and emulsification of fats and waxes in aqueous cleaning solutions (Rosen & Kunjappu 2012), where higher temperatures promote the transition to a mobile oil with decreasing viscosity.

Where latent heat effects are significant, the amount of mobile soil and consequently the rate of removal can be determined by the rate of heat transfer. The spatial location of the phase change presents a moving boundary problem, and the form of the interface depends on the nature of the phase transition, with sharp interfaces associated with the melting of pure components (Hu & Argyropoulos 1996), while diffuse interfaces are associated with mixtures of components. The former are better suited to multi-domain (variable grid, Jana et al. 2007) approaches, where the heat fluxes across the interface are balanced by an enthalpy sink or source term. Continuum approaches, employing temperature dependent heat capacity or enthalpy integration techniques, are often used for the latter, with applications including the mushy transition in metal solidification and in sea ice (Anderson & Gupta 2020) where mass diffusion also plays a role.

## 4. TRANSPORT OF THE SOIL AWAY FROM THE SUBSTRATE

### 4.1. Advection processes

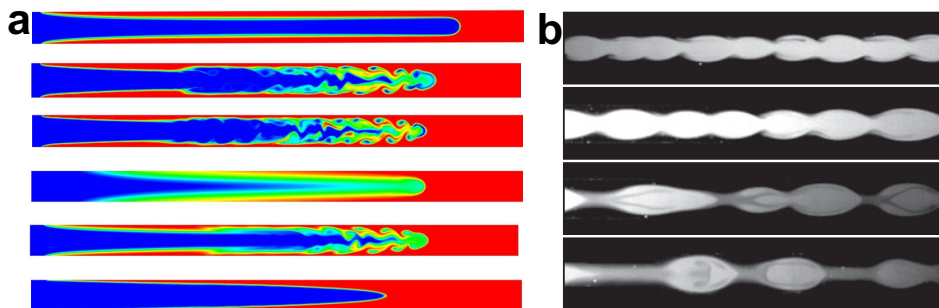


**Figure 8**

Illustrations of interfacial instabilities in multiphase flow displacement in pipes. (a) Newtonian miscible displacement of a more viscous fluid (red, subscript 1) by a less viscous fluid (blue, subscript 2) with same density, flow from left to right, showing the concentration profile. From top to bottom:  $Re = 100$ ,  $Sc = 100$ ,  $\mu_1/\mu_2 = 30$ ;  $Re = 500$ ,  $Sc = 100$ ,  $\mu_1/\mu_2 = 30$ ;  $Re = 1000$ ,  $Sc = 100$ ,  $\mu_1/\mu_2 = 30$ ;  $Re = 500$ ,  $Sc = 1$ ,  $\mu_1/\mu_2 = 25$ ;  $Re = 500$ ,  $Sc = 10$ ,  $\mu_1/\mu_2 = 25$ ;  $Re = 500$ ,  $Sc = 100$ ,  $\mu_1/\mu_2 = 2$ . Adapted with permissions from Sahu et al. (2009) [To request]. (b) Displacement by a less viscous Newtonian fluid (light) of a miscible more viscous Bingham fluid of same density (dark) in an axisymmetric parallel flow with  $\mu_1/\mu_2 = 25$ . Experimental illustration of the transition from the pearl (top) to the mushroom instabilities with, from top;  $Re = 5, 9, 12, 18$ . Adapted with permissions from d’Olce et al. (2008) [To request].

**4.1.1. Bulk displacement.** Mechanical action from the cleanser can drive a flow within the soil, displacing the soil and removing it from the substrate. During the mechanical displacement of a soil by liquid cleanser, instabilities can develop at the cleanser–soil interface, such as: Saffman–Taylor instability (Homsy 1987), shear instabilities (Yih 1967, Boomkamp

& Miesen 1996, Joseph et al. 1997, Craster & Matar 2009), Rayleigh–Taylor instability if the density gradient across the interface is opposed to gravity (Sharp 1984), and capillary instabilities (Eggers 1997). These instabilities can lead to interface deformation, which can modify the forces exerted by the cleanser on the soil. Large deformations of the soil can enhance its removal through roll-up and break-up from the bulk. For instance, in the displacement of a viscous liquid soil initially filling a channel by a less viscous cleanser, a Saffman–Taylor or viscous fingering instability develops (**Figure 8a**). This problem leads to a multilayer parallel flow, which can leave a large fraction of soil on the channel walls. Shear instabilities develop at high Reynolds numbers, inducing vortices and roll-up, which can contribute to the soil displacement, as also shown in **Figure 8a** (Sahu et al. 2009).

In the case of yield-stress soils, *e.g.* cooled waxy crude oils, some personal care products and many foods, other instabilities, such as the pearl and mushroom instabilities (**Figure 8b**) develop depending on  $Re$ , the viscosity ratio and the ratio of the cleanser annular flow radius and the pipe radius (d’Olce et al. 2008). A special case is ice pigging (Quarini 2002), where a viscoplastic slurry of ice particles is pumped through ducts, displacing softer soil ahead of the slurry plug and scouring the duct walls.

Density differences between a soil layer and a cleanser can promote motion when gravity is favourable. Roll-up of otherwise static oils in aqueous solution, driven by dynamic wetting (see Section 3.3), is augmented by density differences. The effect of buoyancy on the stability of immiscible layers of moving liquids has been studied for Newtonian cases (Morgan et al. 2017, Taghavi 2018) and soil layers with more complex rheology (Alba & Frigaard 2016).

Once the bulk of the soil has been displaced by the cleanser flow, a thin film of soil can remain attached to the substrate. Owing to the no-slip boundary condition, viscous forces in the thin film can be large, strongly reducing its removal rate. The displacement of thin films in pipe flows (Yan et al. 1997) or by impinging jets (Yeckel et al. 1990) has been studied extensively in the laminar and turbulent regimes. The lubrication approximation can be used to simplify the governing equations and obtain theoretical predictions for the rate of thinning of the soil film. However, surface roughness can reduce the cleaning rate (Yeckel et al. 1990) and even prevent the removal of soil trapped in cavities separated from the main flow (Yan et al. 1997), particularly for immiscible soils.

When the soil left on the substrate is in the form of small patches or droplets, the displacement of the soil strongly depends on the contact line dynamics. The difficulties in modelling the motion of the contact line (see Section 1.2) can affect the accuracy with which the rate of removal of soil and appearance of clean substrate is calculated. In the case of immiscible droplets in a shear flow, theoretical asymptotic studies assume that droplets start moving on a substrate when the contact angle due to deformation is larger than the advancing contact angle at the front of the droplet and smaller than the receding contact angle at its rear (**Figure 3a**) (Dussan V. 1987). Numerical simulations have been able to refine asymptotic results to determine the onset of drop displacement for a range of capillary numbers ( $Ca = \mu U/\gamma$ ), contact angles and contact angle hysteresis, viscosity ratios, Bond number and drop size (Dimitrakopoulos & Higdon 1997), as well as in the presence of surfactant (Schleizer & Bonnecaze 1999). Experiments (Le Grand et al. 2005) have shown that in the regime where the drop remains a coherent body and for uniform, chemically homogeneous substrates, the model predictions are accurate. However, the drop can break up or shed smaller droplets at the rear, displaying qualitatively different regimes.

**4.1.2. Advection–diffusion transport of dissolved soil.** Once the soil is dissolved in the cleanser it can be transported in the cleanser flow, following an advection–diffusion equation such as Equation 1. The relative importance between advection and diffusion is characterised by the Péclet number:  $Pe = UL/D$ , with  $D$  the diffusivity of the soil in the cleanser. At large  $Pe$ , the advection–diffusion equation becomes singular and the concentration field possess a thin boundary layer at the cleanser–soil interface where the mass transfer occurs. Convective mass transfer problems are related to heat transfer problems as heat and mass follow similar advection–diffusion equations, provided they can be both considered as passive tracers (Gekas & Hallström 1987). This approximation is generally valid in the dilute concentration limit, such that the dissolved mass does not affect other quantities in the problem. Otherwise, additional constitutive equations may be required to model, for instance, the impact of mass on the viscosity of the mixture. This introduces additional non-linearities in the advection–diffusion equation and couples this equation with that for momentum conservation, Equation 3, thereby rendering the problem more complex. The added mass can also affect the local density of the mixture, which can induce positive or negative buoyancy effects under gravity, or inertial effects.

Since the pioneering work of Graetz (1885), advances in convective mass transfer problems have benefited from progress in convective heat transfer. One of the most important quantities sought is the local mass transfer flux per unit area of cleanser–soil interface. This interfacial mass flux depends on the concentration gradient at the interface and is often modelled using a convective mass transfer coefficient  $k$  (Bejan 2013) and an overall concentration difference. The non-dimensional convective mass transfer coefficient, the Sherwood number,  $Sh = kL/D$ , is analogous to the Nusselt number in heat transfer. It is typically modelled following (Gekas & Hallström 1987),

$$Sh \propto Re^\alpha Sc^\omega (d_h/L)^\delta, \quad 11.$$

with  $Sc = \nu/D$  the Schmidt number,  $d_h$  the hydraulic diameter of the domain, and  $\alpha$ ,  $\omega$  and  $\delta$  three exponents, typically between 0 and 1, which have been determined theoretically for simple laminar flows and empirically otherwise. The exponents and functional relationships differ for laminar and turbulent flows. The model Equation 11 has been applied in the decontamination of droplets dissolving in a shear flow in two-dimensional (Landel et al. 2015, 2016, and references therein) and three-dimensional problems (Etzold et al. 2020).

One of the key differences between heat and mass transfer is that the latter often leads to a time-dependent evolution of the cleanser–soil interface. The interfacial instabilities discussed in Section 4.1.1, in combination with soil miscibility with the cleanser, can enhance mass transfer through an increase in interfacial area (Hanratty 1981). As  $Pe$  decreases, the interface also becomes more diffuse (see green-yellow concentration field in **Figure 8a**, which shows diffusive mixing between the red and blue substances). The combination of strong deformation and diffusion makes the interface difficult to track. This is best captured through high-resolution numerical simulations (Sahu et al. 2009) or experiments (d’Olce et al. 2008). A second difference, mentioned in Section 1.1, is that Fick’s first law (and, as a result, the Sherwood–Nusselt analogy) may not apply and more detailed models are required to evaluate the mass fluxes.

**4.1.3. Particulate displacement.** Particles immersed in a moving liquid film can slide or roll along a surface, or be lifted from the surface, by the combination of torque, translation and lifting hydrodynamic forces (Hubbe 1994). Both viscous and turbulent (Soltani & Ahmadi

2012) wall layers have been considered, the latter featuring ‘turbulent bursts’ which provide additional removal mechanisms, countering particulate deposition (Guha 2008). Much of the literature on calculating the normal forces and torque features individual spherical particles on flat substrates: viscous flow around spherical entities has been considered by Pozrikidis (1997) and Gaver & Kute (1998), and non-spherical entities, *e.g.* bacterial cells by Bouklas & Huang (2012). Other factors include the effect of roughness (Nasr et al. 1994), which evolves as particulate material is removed. Particles are often present in the form of beds and saltation — the intermittent motion of particles from granular beds — is reviewed by Ali & Dey (2019).

Detachment and displacement occur when the hydrodynamic forces exceed the adhesion forces (Sharma et al. 1992). The adhesion of spores, cells and biofilms is a dynamic phenomenon involving several mechanisms (Carniello et al. 2018). The challenge in cleaning studies is to identify which adhesion phenomena are active, and quantifying the strength of the interactions. When the soils are multiphase, this can be challenging. Consider the four-phase case shown in **Figure 3c**, involving a particle immersed in cleanser where a secondary liquid phase (in orange), which is immiscible with the cleanser, wets both the substrate and soil particle. The secondary liquid forms liquid bridges between particles and between particles and the substrate, increasing the cohesive and adhesive forces, respectively. Examples of such systems arise in EOR applications, soil remediation and dishwashing. If the continuous phase is air, a small amount of wetting secondary liquid is sufficient to induce plastic behaviour, exploited in building sandcastles.

Capillary attractions are exploited in self-cleaning surfaces, where a droplet of cleanser which is non-wetting towards the substrate but wetting towards the particulate soil phase can pull smaller particles off an otherwise dry substrate (**Figure 3d**) (Hassan et al. 2019). By matching the properties of the particles, substrate and cleanser, and suitably sized droplets, sprays can be used to clean small particles off dusty surfaces.

Submerged droplets can also be displaced by a shear flow, particularly if the droplet phase is non-wetting. The shear flow will also change the droplet shape if  $Ca$  is sufficiently large. Droplet deformation and detachment has been considered by Gupta and co-workers (Gupta 1997, Gupta & Basu 2008).

## 4.2. Diffusive processes

In some systems, the overall cleaning or decontamination rate may be low due to the removal rate being limited by slow diffusion processes, as typically found in porous materials (Section 2.4). This can also occur in systems where advection may be strong in some parts but diffusion dominates in others. Confined spaces such as narrow gaps, micro-channels and pores can considerably reduce advection processes (Etzold et al. 2020). The local  $Pe$  is typically very small. Diffusion also controls the mass transfer across flow separation surfaces in the cleanser phase (Section 2.1), even though  $Pe$  may be large near the separatrix.

Landel et al. (2016) studied the removal of traces of soil miscible in a cleanser and contained in polymer-thickened droplets attached to a substrate. They found that even when  $Pe$  in the cleanser flow over the droplets was large, the removal rate was still limited by diffusion within the droplet. The polymer inside the droplet strongly reduced advection for both the cleanser and the soil. They also showed that if internal advection inside the droplet could be increased, for instance by a shear-induced recirculation in the droplet, the removal rate of the soil would increase noticeably.

Dalwadi et al. (2017) studied the reactive decontamination of a chemical agent in porous media which moved under diffusion alone, i.e. with  $\mathbf{u} = 0$  in Equation 1. For a chemical agent immiscible in the cleanser, they showed that increasing the partition coefficient  $\kappa$  of the reaction products in the cleanser enhanced the decontamination rate. There are strong overlaps with chemical reactor theory in this area (Fogler 2020).

In the cleaning of fibrous materials, such as cloths, advection in the cleanser flow is not strong enough to remove soil from small pores within the fabric. Shin et al. (2018) showed that diffusiophoresis is the main mechanism driving soil out of the pores. Diffusiophoresis is the motion of colloids or molecules induced by the concentration gradient from another solute (Moran & Posner 2017). In fabric washing, the concentration gradient is established during the rinsing process, leaving fabric pores saturated with detergent, whilst the detergent is washed away outside the pores. The resulting gradient in detergent concentration moves soil trapped in the pores through diffusiophoresis. Soil is removed from these pores at a higher rate than under self-diffusion alone.

## 5. SUMMARY

### SUMMARY POINTS

1. C&D of soils at surfaces by a liquid cleanser is a complex multiphase and multi-physics problem involving a broad range of time and length scales.
2. C&D can be modelled by governing equations describing the physics and chemistry of the flow in the cleanser and soil phases, the dynamics of the cleanser–soil–substrate interfaces and the three-phase contact line.
3. C&D applications using liquid cleansers follow three stages, where fluid mechanics plays an important role: (i) the flowing cleanser must reach and contact the soil, (ii) the cleanser performs a cleaning action or transports a cleaning agent, (iii) the cleanser transports the soil away from the substrate.
4. This is a rich, time-dependent problem, where instabilities, particularly at the interface, can occur, modifying the cleaning action and removal of the soil. Many applications involve moving boundary problems, where the distribution of components and location of interfaces evolve spatially and temporally. Where removal is slow the fluxes can be modelled as a quasi-stationary problem and integrated over time. Rapid removal presents challenges in solving the fully coupled problem.
5. Chemical, surfactant and temperature actions can change the properties of the different phases or the physical phenomena involved, thereby modify the governing equations (and dynamics) substantially. These factors can enhance the overall C&D rate and effectiveness.

### FUTURE ISSUES

1. Numerical models require accurate physical property and transport parameter data. These could be obtained by new measurements or by revisiting earlier studies.
2. Scale-up introduces complexity associated with changes in phenomena controlling behaviour at different length scales and extended time scales, and variation of pa-

rameters across large spatial systems. This is important when relating laboratory results to applications.

3. For soils with complex rheology and time-dependent behaviour, appropriate constitutive models capturing the behaviour manifested during cleaning operations need to be identified. Solution methods for these models may not currently exist.
4. Contact line dynamics are challenging to capture and model accurately for realistic substrates, whether experimentally, numerically or theoretically.
5. Interfacial dynamics are similarly challenging owing to large gradients in key quantities (velocity, density, concentration) and the development of instabilities.
6. The adhesion forces between the soil and substrate, in static and dynamic equilibrium, are difficult to measure and predict, yet are crucial for modelling removal.

## DISCLOSURE STATEMENT

The authors are not aware of any affiliations, memberships, funding, or financial holdings that might be perceived as affecting the objectivity of this review.

## ACKNOWLEDGEMENTS

Conversations and discussions on C&D topics with many colleagues and particularly the members of the UK Fluids Network Special Interest Group 10 (Fluid Mechanics of C&D) are gratefully acknowledged.

## References

- Alba K, Frigaard IA. 2016. Dynamics of the removal of viscoplastic fluids from inclined pipe. *J. Non-Newton. Fluid Mech.* 229:43–58
- Ali SZ, Dey S. 2019. Bed particle saltation in turbulent wall-shear flow: a review. *Proc. Roy. Soc. A.* 475:20180824
- Anderson DM, Gupta P. 2020. Convective phenomena in mushy layers. *Annu. Rev. Fluid Mech.* 52:93–119
- Aouad W, Landel JR, Davidson JF, Dalziel SB, Wilson DI. 2016. Particle image velocimetry and modelling of horizontal coherent liquid jets impinging on and draining down a vertical wall. *Exp. Therm. Fluid Sci.* 74:429–443
- Balmforth NJ, Frigaard IA, Ovarlez G. 2014. Yielding to stress: Recent developments in viscoplastic fluid mechanics. *Annu. Rev. Fluid Mech.* 46:121–146
- Bejan A. 2013. Convection Heat Transfer. Wiley, 4th ed.
- Bhagat RK, Jha NK, Linden PF, Wilson DI. 2018. On the origin of the hydraulic jump in a thin liquid film. *J. Fluid Mech.* 851:R5
- Bhagat RK, Wilson DI. 2016. Flow in the thin film created by a coherent turbulent water jet impinging on a vertical wall. *Chem. Eng. Sci.* 152:606–623
- Bird RB, Stewart WE, Lightfoot EN. 2002. Transport Phenomena. John Wiley & Sons, 2nd ed.
- Bird RB, Wiest JM. 1995. Constitutive equations for polymeric liquids. *Annu. Rev. Fluid Mech.* 27:169–93
- Bonn D, Eggers J, Indekeu J, Meunier J, Rolley E. 2009. Wetting and spreading. *Rev. Mod. Phys.* 81:739–805
- Boomkamp PAM, Miesen RHM. 1996. Classification of instabilities in parallel two-phase flow. *Int. J. Multiphase Flow* 22:67–88

- Bouklas B, Morchain J, Mercier Bonin M, Janel S, Lafont H, Schmitz P. 2012. A combined computational fluid dynamics (CFD) and experimental approach to quantify the adhesion force of bacterial cells attached to a plane surface. *Soft Matter* 8:8194
- Bouklas N, Huang R. 2012. Swelling kinetics of polymer gels: comparison of linear and non-linear theories. *AIChE J.* 58:3614–3624
- Carniello V, Peterson BW, van der Mei HC, Busscher J. 2018. Physico-chemistry from initial bacterial adhesion to surface-programmed biofilm growth. *Adv. Colloid Interf. Sci.* 261:1–14
- Carroll BJ. 1981. The kinetics of solubilization of nonpolar oils by nonionic surfactant solutions. *J. Colloid Interface Sci.* 79:126–135
- Carroll BJ. 1993. Physical aspects of detergency. *Colloid. Surface. A* 74:131–167
- Chang HC. 1994. Wave evolution on a falling film. *Annu. Rev. Fluid Mech.* 26:103–136
- Chang K, Constantinescu G, Park SO. 2018. Analysis of the flow and mass transfer processes for the incompressible flow past an open cavity with a laminar and a fully turbulent incoming boundary layer. *J. Fluid Mech.* 561:113–145
- Chee MWL, Ahuja TV, Bhagat RK, Taesopapong N, Wan SA, et al. 2019. Effect of jet length and wall curvature on cleaning of tank walls. *Food Bioprod. Proc.* 113:142–153
- Chen S, Bertola V. 2017. Morphology of viscoplastic drop impact on viscoplastic surfaces. *Soft Matter* 13:711
- Craster RV, Matar OK. 2009. Dynamics and stability of thin liquid films. *Rev. Mod. Phys.* 81:1131–1198
- Cutler WG, Kissa A, eds. 1986. Detergency: Theory and technology. Marcel Dekker, New York
- Dalwadi MP, O’Kiely D, Thomson SJ, Khaleque TS, Hall CL. 2017. Mathematical modeling of chemical agent removal by reaction with an immiscible cleanser. *SIAM J. Appl. Math.* 77:1937–1961
- Dimitrakopoulos P, Higdon JJJ. 1997. Displacement of fluid droplets from solid surfaces in low-reynolds-number shear flows. *J. Fluid Mech.* 336:351–378
- Douay CL, Faure TM, Lusseyran F. 2013. Stereoscopic PIV using optical flow: application to a cavity recirculation. *Exp. Fluids* 54:1579
- Dussan V. EB. 1979. On the spreading of liquids on solid surfaces: static and dynamic contact lines. *Annu. Rev. Fluid Mech.* 11:371–400
- Dussan V. EB. 1987. On the ability of drops to stick to surfaces of solids. part 3. the influences of the motion of the surrounding fluid on dislodging drops. *J. Fluid Mech.* 174:381–397
- d’Olce M, Martin J, Rakotomalala N, Salin D, Talon L. 2008. Pearl and mushroom instability patterns in two miscible fluids’ core annular flows. *Phys. Fluids* 20:024104
- Eggers J. 1997. Nonlinear dynamics and breakup of free-surface flows. *Rev. Mod. Phys.* 69:865–929
- Etzold MA, Landel JR, Dalziel SB. 2020. Three-dimensional advective–diffusive boundary layers in open channels with parallel and inclined walls. *Int. J. Heat Mass Tran., in press*
- Fang LC. 2003. Effect of mixed convection on transient hydrodynamic removal of a contaminant from a cavity. *Int. J. Heat Mass Tran.* 46:2039–2049
- Fogler HS. 2020. Elements of Chemical Reaction Engineering. Prentice-Hall, 5th ed.
- Fryer PJ, Asteriadiou K. 2009. A prototype cleaning map: a classification of industrial cleaning processes. *Trends Food Sci. Tech.* 20:255–262
- Gaver DP, Kute SM. 1998. A theoretical model study of the influence of fluid stresses on a cell adhering to a microchannel wall. *Biophys. J.* 75:721–733
- Gekas V, Hallström B. 1987. Mass transfer in the membrane concentration polarization layer under turbulent cross flow I. Critical literature review and adaptation of existing Sherwood correlations to membrane operations. *Journal of Membrane Science* 30:153–170
- Glover HW, Brass T, Bhagat RK, Davidson JF, Pratt L, Wilson DI. 2016. Cleaning of complex soil layers on vertical walls by fixed and moving impinging liquid jets. *J. Food Eng.* 178:95–109
- Gorokhovski M, Herrmann M. 2008. Modeling primary atomization. *Annu. Rev. Fluid. Mech.* 40:311–341

- Graetz L. 1885. Über die Wärmeleitungsfähigkeit von Flüssigkeiten. *Annalen der Physik* 261:337–357
- Guha A. 2008. Transport and deposition of particles in turbulent and laminar flow. *Annu. Rev. Fluid. Mech.* 40:343–366
- Guha A, Barron RM, Balachandar R. 2011. An experimental and numerical study of water jet cleaning process. *J. Mater. Process. Tech.* 211:610–618
- Gupta AK. 1997. A model for detachment of a partially wetting drop from a solid surface by shear flow. *J. Colloid Interf. Sci.* 190:253–257
- Gupta AK, Basu S. 2008. Deformation of an oil droplet on a solid substrate in simple shear flow. *Chem. Eng. Sci.* 63:5496–5502
- Hanratty TJ. 1981. Stability of surfaces that are dissolving or being formed by convective diffusion. *Annu. Rev. Fluid Mech.* 13:231–52
- Hartley DE, Murgatroyd W. 1964. Criteria for the break-up of thin liquid layers flowing isothermally over solid surfaces. *Int. J. Heat Mass Tran.* 7:1003–1015
- Hassan G, Yilbas BS, Al-Sharafi A, Al-Qahtan H. 2019. Self-cleaning of a hydrophobic surface by a rolling water droplet. *Sci. Rep.* 9:5744
- Higdon JLL. 1985. Stokes flow in arbitrary two-dimensional domains: shear flow over ridges and cavities. *J. Fluid Mech.* 159:195–226
- Homsy GM. 1987. Viscous fingering in porous media. *Annu. Rev. Fluid Mech.* 19:271–311
- Horner M, Metcalfe G, Wiggins S, Ottino JM. 2002. Transport enhancement mechanisms in open cavities. *J. Fluid Mech.* 452:199–229
- Hsu TT, Walker TW, Frank CW, Fuller GG. 2011. Role of fluid elasticity on the dynamics of rinsing flow by an impinging jet. *Phys. Fluids.* 23:033101
- Hu H, Argyropoulos SA. 1996. Mathematical modelling of solidification and melting: A review. *Model. Sim. Mat. Sci. Eng.* 4:371–39
- Hubbe MA. 1994. Theory of detachment of colloidal particles from flat surfaces exposed to flow. *Colloid Surf.* 12:151–178
- Hunek B, Cussler EL. 2002. Mechanisms of photoresist dissolution. *AIChEJ* 48:661–672
- Israelachvili JN. 2011. Intermolecular and Surface Forces. San Diego: Academic Press, 3rd ed.
- Jameson GJ, Jenkins CE, Button EC, Sader JE. 2010. Water bells formed on the underside of a horizontal plate. part 1. experimental investigation. *J. Fluid Mech.* 649:19–43
- Jana S, Ray S, Durst F. 2007. A numerical method to compute solidification and melting processes. *Appl. Math. Model.* 31:93–119
- Joseph DD, Bai R, Chen KP, Renardy YY. 1997. Core-annular flows. *Annu. Rev. Fluid Mech.* 29:65–90
- Jung S, Hutchings IM. 2012. The impact and spreading of a small liquid drop on a non-porous substrate over an extended time scale. *Soft Matter* 8:2686–2696
- Kahler DM, Kabala Z. 2016. Acceleration of groundwater remediation by deep sweeps and vortex ejections induced by rapidly pulsed pumping. *Water Resour. Res.* 52:3930–3940
- Kibar A, Karaby H, Yigit KS, Ucar IO, Erbil HY. 2010. Experimental investigation of inclined liquid water jet flow onto vertically located superhydrophobic surfaces. *Exp. Fluids* 49:1135–1145
- Kim JY, Hwang IG, Weon BM. 2017. Evaporation of inclined water droplets. *Sci. Rep.* 7:42848
- Kondo T, Ando K. 2019. Simulation of high-speed droplet impact against a dry/wet rigid wall for understanding the mechanism of liquid jet cleaning. *Pys. Fluids* 31:013303
- Landel JR, McEvoy H, Dalziel SB. 2015. Cleaning of viscous drops on a flat inclined surface using gravity-driven film flows. *Food Bioprod. Proc.* 93:310 – 317
- Landel JR, Thomas AL, McEvoy H, Dalziel SB. 2016. Convective mass transfer from a submerged drop in a thin falling film. *J. Fluid Mech.* 789:630–668
- Le Grand N, Daerr A, Limat L. 2005. Shape and motion of drops sliding down an inclined plane. *J. Fluid Mech.* 541:293–315
- Li D, Kang Y, Ding X, Liu W. 2017. Effects of the geometry of impinging surface on the pressure

- oscillations of self-resonating pulsed waterjet. *Adv. Mech. Eng.* 9:1–11
- Lin SP, Reitz RD. 1998. Drop and spray formation from a liquid jet. *Annu. Rev. Fluid Mech.* 30:85–105
- Mabrouki T, Raissi K, Cornier A. 2000. Numerical simulation and experimental study of the interaction between a pure high-velocity waterjet and targets: contribution to investigate the decoating process. *Wear.* 239:260–273
- Mackay DM, Wilson RD, Brown MJ, Ball WP, Xia G, Durfee DP. 2000. A controlled field evaluation of continuous vs. pulsed pump-and-treat remediation of a voc-contaminated aquifer: site characterization, experimental setup, and overview of results. *J. Contam. Hydrol.* 41:81–131
- Markl D, Yassin S, Wilson DI, Goodwin DJ, Anderson A, Zeitler JA. 2017. Mathematical modelling of liquid transport in swelling pharmaceutical immediate release powder compacts. *Int. J. Pharm.* 526:1–10
- Melo LF, Bott TR. 1997. Biofouling in water systems. *Exp. Therm. Fluid Sci.* 14:375–381
- Mertens K, Putkaradze V, Vorobieff P. 2005. Morphology of a stream flowing down an inclined plane. part 1. braiding. *J. Fluid Mech.* 531:49–58
- Miller-Chou BA, Koenig JL. 2003. A review of polymer dissolution. *Prog. Polymer Sci.* 28:1223–1270
- Mitchell BR, Klewicki JC, Korkolis YP, Kinsey BL. 2019. Normal impact force of Rayleigh jets. *Phys. Rev. Fluid* 4:113603
- Moffatt HK. 1964. Viscous and resistive eddies near a sharp corner. *J. Fluid Mech.* 18:1–18
- Moran JL, Posner JD. 2017. Phoretic self-propulsion. *Annu. Rev. Fluid Mech.* 49:511–540
- Morgan RG, Ibarra R, Zadrazil I, Matar OK, Hewitt GF, Markides CN. 2017. On the role of buoyancy-driven instabilities in horizontal liquid–liquid flow. *Int. J. Multiphase Flow* 89:123–135
- Nasr B, Ahmadi G, Ferro AR, Dhaniyala S. 1994. A model for particle removal from surfaces with large-scale roughness in turbulent flows. *Aerosol Sci. Tech.* 54:291–303
- Nishimura T, Kunitsugu K. 1997. Fluid mixing and mass transfer in two-dimensional cavities with time-periodic lid velocity. *Int. J. Heat Fluid Flow* 18:497–506
- NRC NRC. 1994. Alternatives for Ground Water Cleanup. Washington, DC: The National Academies Press
- Payatakes AC. 1982. Dynamics of oil ganglia during immiscible displacement in water-wet porous media. *Annu. Rev. Fluid Mech.* 14:365–393
- Perazzo CA, Gratton JS. 2004. Navier-Stokes solutions for parallel flow in rivulets on an inclined plane. *J. Fluid Mech.* 507:367–379
- Pozrikidis C. 1997. Shear flow over a protuberance on a plane wall. *J. Eng. Math.* 31:29–42
- Prosperetti A. 1979. Boundary conditions at a liquid–vapor interface. *Meccanica* 14:34–47
- Prosser AJ, Franses EI. 2001. Adsorption and surface tension of ionic surfactants at the air–water interface: review and evaluation of equilibrium models. *Colloids Surf. A* 178:1–40
- Quarini J. 2002. Ice-pigging to reduce and remove fouling and to achieve clean-in-place. *Appl. Thermal Eng.* 22:747–753
- Rosen MJ, Kunjappu JT. 2012. Surfactants and Interfacial Phenomena. John Wiley & Sons, 4th ed.
- Sahu KC, Ding H, Valluri P, Matar OK. 2009. Linear stability analysis and numerical simulation of miscible two-layer channel flow. *Phys. Fluids* 21:042104
- Schleizer AD, Bonnecaze RT. 1999. Displacement of a two-dimensional immiscible droplet adhering to a wall in shear and pressure-driven flows. *J. Fluid Mech.* 383:29–54
- Schott H. 1992. Swelling kinetics of polymers. *J. Mac. Sci. Phys. B* 31:1–9
- Sethi SK, Manik G. 2018. Recent progress in super hydrophobic/hydrophilic self-cleaning surfaces for various industrial applications: A review. *Poly. Plastics Tech. Eng.* 57:1932–1952
- Shankar PN, Deshpande MD. 2000. Fluid mechanics in the driven cavity. *Annu. Rev. Fluid Mech.* 32:93–136
- Sharma MM, Chamoun H, Sarma DSHSR, Schechter RS. 1992. Factors controlling the hydrodynamic

- detachment of particles from surface. *J. Colloid Interf. Sci.* 149:121–134
- Sharp DH. 1984. An overview of Rayleigh–Taylor instability. *Physica D* 12:3–18
- Shin S, Warren PB, A SH. 2018. Cleaning by Surfactant Gradients: Particulate Removal from Porous Materials and the Significance of Rinsing in Laundry Detergency. *Phys. Rev. Appl.* 9:034012
- Smith ER, Theodorakis PE, Craster RV, Matar OK. 2018. Moving contact lines: linking molecular dynamics and continuum-scale modeling. *Langmuir* 34:12501–12518
- Snoeijer JH, Andreotti B. 2013. Moving contact lines: scales, regimes, and dynamical transitions. *Annu. Rev. Fluid Mech.* 45:269–292
- Soltani M, Ahmadi G. 2012. On particle adhesion and removal mechanisms in turbulent flows. *J. Adhesion Sci. Tech.* 8:763–785
- Sui Y, Ding H, Spelt PDM. 2014. Numerical simulations of flows with moving contact lines. *Annu. Rev. Fluid Mech.* 46:97–119
- Taghavi SM. 2018. A two-layer model for buoyant displacement flows in a channel with wall slip. *J. Fluid Mech.* 852:602–640
- Tatekura M, Watanabe M, Kobayashi K, T S. 2018. Pressure generated at the instant of impact between a liquid droplet and solid surface. *R. Soc. open sci.* 5:181101
- Thampi SP, Pagonabarraga I, Adhikari R, Govindarajan R. 2016. Universal evolution of a viscous–capillary spreading drop. *Soft Matter* 12:6073
- Theofanous TG. 2011. Aerobreakup of newtonian and viscoelastic liquids. *Annu. Rev. Fluid Mech.* 43:661–690
- Tsiartas PC, Flanagan LW, Henderson CL, Hinsberg WD, Sanchez IC, et al. 1997. The mechanism of phenolic polymer dissolution: A new perspective. *Macromolecules.* 30:4656–4664
- Vaezi. 2015. Experimental investigation of elastic properties effects on viscous fingering instability. Master’s thesis, Shahrood University of Technology
- Walker TW, Hsu TT, Frank CW, Fuller GG. 2012. Role of shear-thinning on the dynamics of rinsing flow by an impinging jet. *Phys. Fluids* 24:093102
- Wang S, Li Z, Liu B, Zhang X, Yang Q. 2015. Molecular mechanisms for surfactant-aided oil removal from a solid surface. *Appl. Surf. Sci.* 359:98–105
- Wilson DI. 2005. Challenges in cleaning: Recent developments and future prospects. *Heat Transfer Eng.* 26:51–59
- Wooding RA, Morel-Seytoux HJ. 1976. Multiphase fluid flow through porous media. *Annu. Rev. Fluid Mech.* 8:233–274
- Xin H, Chen XD, Ozkan N. 2004. Removal of a model protein foulant from metal surface. *AIChE J.* 50:1961–1973
- Yan JF, Eduardo Sáez A, Grant CS. 1997. Removal of oil films from stainless steel tubes. *AIChE J.* 43:251–259
- Yarin AL. 2006. Drop impact dynamics: Splashing, spreading, receding, bouncing. *Annu. Rev. Fluid Mech.* 38:159–192
- Yazdi AA, Norouzi M. 2018. Numerical study of saffman–taylor instability in immiscible nonlinear viscoelastic flows. *Rheol. Acta* 57:575–589
- Yeckel A, Middleman S, Klumb LA. 1990. The removal of thin liquid films from periodically grooved surfaces by an impinging jet. *Chem. Eng. Commun.* 96:69–79
- Yeckel JF, Strong L, Middleman S. 1994. Viscous film flow in the stagnation region of the jet impinging on planar surface. *AIChE J.* 40:1611–1617
- Yih CS. 1967. Instability due to viscosity stratification. *J. Fluid Mech.* 27:337–352
- Zhao B, MacMinn CW, Juanes R. 2016. Wettability control on multiphase flow in patterned microfluidics. *P. Natl. Acad. Sci. USA* 113:10251–10256
- Zohourkari I, Zohoor M, Annoni M. 2014. Investigation of the effects of machining parameters on material removal rate in abrasive waterjet turning. *Adv. Mech. Eng.* 6:624203